

Chaotic Feature in the Light Curve of 3C 273

Lei Liu

Institute of Particle Physics, Huazhong Normal University, Wuhan 430079; liuphy@mail.ccnu.edu.cn

Received 2006 March 9; accepted 2006 May 31

Abstract Some nonlinear dynamical techniques, including state-space reconstruction and correlation integral, are used to analyze the light curve of 3C 273. The result is compared with a chaotic model. The similarities between them suggest there is a low-dimension chaotic attractor in the light curve of 3C 273.

Key words: galaxies: active — galaxies: individual: 3C 273

1 INTRODUCTION

Since the discovery by Smith & Hoffleit (1963), the light curve of 3C 273 has played an important role in our understanding of the nature of the quasar. Although it has been subjected to extensive analysis, there is no generally accepted method of extracting the information in the light curve. Results of analysis of the light curve ranged from a multi-periodic behavior (Kunkel 1967; Jurkevich 1971; Sillanpaa et al. 1988; Lin 2001) to a purely random process (Manwell & Simon 1966, 1968; Terrell & Olsen 1970; Fahlman & Ulrych 1975). Whatever does this *seemingly* random light curve tell us? Could this seeming randomness be some behaviour other than multi-periodic or purely random?

In 1963, Edward Lorenz published his monumental work entitled *Deterministic Nonperiodic Flow*. In this paper, he found a strange behavior which can appear in a deterministic nonlinear dissipative system, which seems random and unpredictable, and is called *Chaos*. Chaotic behavior is not multi-periodic because it has a continuous spectrum. Useful information can not always be extracted from the power spectrum of chaotic signal. On the other hand chaotic behavior is not random either because it can appear in a completely deterministic system. The concept of *attractor* is often used when describing chaotic behaviors. As the dissipative system evolves in time, the trajectory in state space may head for some final region called attractor. The attractor may be an ordinary Euclidean object or a fractal (Feder 1988) which has a non-integer dimension and often appears in the state space of a chaotic system. For many practical systems, we may not know in advance the required degrees of freedom and hence can not measure all the dynamic variables. How can we discern the nature of the attractor from the available experimental data? Packard et al. (1980) introduced a technique which can be used to reconstruct state-space attractor from the time series data of a *single* dynamical variable. Moreover, an algorithm subsequently introduced by Grassberger & Procaccia (1983) can be used to determine the dimension of the attractor embedded in the new state space. These techniques constitute a useful diagnostic method of chaos in practical systems.

3C 273 may be a complex nonlinear dissipative system. If so, the complex light variation of 3C 273 can be chaotic. Here we use the techniques introduced by Packard et al. (1980) and Grassberger et al. (1983) to investigate whether there is a chaotic attractor in the light curve of 3C 273. The paper is arranged as follows: In Section 2 a brief introduction to the method for diagnosing chaos is presented. In Section 3 we apply this method to a chaotic model and 3C 273 and then compare the results. In Section 4 a discussion is given.

2 METHOD OF ANALYSIS

The state-space reconstruction technique (Packard et al. 1980) which is based on the notion that the attractor of a multi-dimensional dissipative system can often be reconstructed from the time series data of a *single*

variable. Since a detailed presentation of this technique is available in many places (see, e.g., Hilbron 1994; Abarbanel et al. 1993; Sprott 2003), we just give a brief introduction here. Let X_1, X_2, \dots, X_N be measurements of a physical variable at times $t_i = t_0 + (i - 1)\Delta t, i = 1, \dots, N$. From this sequence one can construct a set of d -dimensional vectors $\mathbf{v}_i, i = 1, \dots, N - (d - 1)T$ of the form

$$\mathbf{v}_i = (X_i, X_{i+T}, X_{i+2T}, \dots, X_{i+(d-1)T}), \quad (1)$$

where T , called the *time delay*, is an integral multiple of Δt . We assume that the real attractor in the full state space of the system can be reconstructed from the time-delayed vectors \mathbf{v}_i moving in the d -dimensional state space, d is often called *embedding dimension*. This assumption works well when the embedding dimension is greater than about twice the dimension of the real attractor (Sprott 2003).

The correlation integral (Grassberger & Procaccia 1983; see also Hilbron 1994; Abarbanel et al. 1993; Sprott 2003) can be used to determine the attractor dimension, defined as

$$C(r) = \frac{1}{(N - k)(N - k - 1)} \sum_{i=1}^{N-k} \sum_{j=1, j \neq i}^{N-k} \theta(r - |\mathbf{v}_i - \mathbf{v}_j|), \quad (2)$$

where $k = (d - 1)T$, and $\theta(x)$ is the Heaviside function,

$$\theta(x) = \begin{cases} 1 & x \geq 0, \\ 0 & x < 0. \end{cases} \quad (3)$$

For the dissipative system, $C(r)$ behaves as a power of r for r small,

$$C(r) \propto r^D, \quad (4)$$

where D is called the *correlation dimension*. Strictly D is not the attractor dimension, but is very close to it (Grassberger & Procaccia 1983). Thus attractor dimension can be estimated from the correlation dimension. Note that for large values of r the finite size of the attractor makes $C(r)$ “saturate” at 1, while for small values of r the finite number of data points causes $C(r)$ to be close to zero. Thus, the curve of $\log_{10} C(r)$ versus $\log_{10} r$ is approximately a straight line just in the intermediate region. See Figure 1.

What we first do in practice is to compute the correlation dimension D by using Equations (2) and (4). As the value of D depends on the delay time T and the embedding dimension d , we plot D versus d for different values of T , as in Figure 2. If there is a chaotic attractor, D should be independent of d until d becomes greater than some value defined by d_{sat} . For some special value of T , d_{sat} is about twice the value of saturation correlation dimension D_{sat} , that is the value independent of d (Sprott 2003). Thus, the saturation dimension D_{sat} which corresponds to this special value of T is the attractor dimension that we wish to find from the single time series data.

3 DATA ANALYSIS

First, we apply the method described above to the Lorenz model introduced by Lorenz (1963) to model the convection in the atmosphere. It treats the fluid system (the atmosphere) as a fluid layer that is heated at the bottom (the sun heats the earth’s surface, for example) and cooled at the top. A detailed derivation of the equations of the Lorenz model can also be found in many textbooks (see, e.g., Hilbron 1994). Here we just give the result,

$$dx/dt = \sigma(y - x), \quad (5)$$

$$dy/dt = -xz + \gamma x - y, \quad (6)$$

$$dz/dt = xy - bz. \quad (7)$$

It is important to stress that the Lorenz model introduced here is not treated as a model of 3C 273. We just use it to produce a set of chaotic time series and show what would happen when the method of chaos diagnosis is used to analyze a set of chaotic time series. We choose the parameters $\sigma = 10, \gamma = 28$ and $b = 8/3$ which are used by many authors to produce a set of chaotic solution of Lorenz equations. We use the order-4 Runge-Kutta method to solve the equations with the initial conditions $x_0 = 0, y_0 = -0.01, z_0 = 9$,

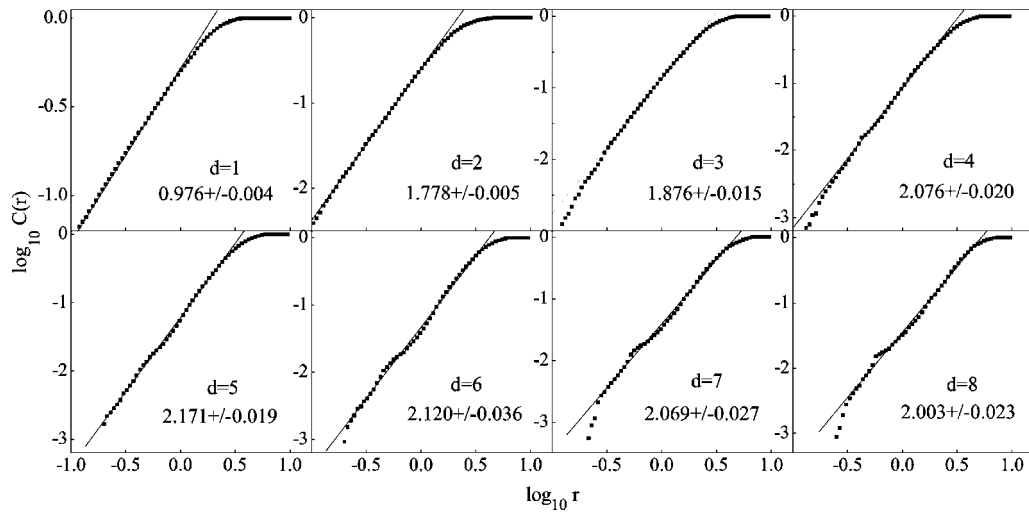


Fig. 1 Correlation integral $C(r)$ of Lorenz model for time delay $T = 20$ and embedding dimension $d = 1, 2, \dots, 8$ on doubly logarithmic scales. In each panel the scale of $C(r)$ is arbitrary and the scale of r is the same. We also give the slope fitted by using Eq. (4) in each panel.

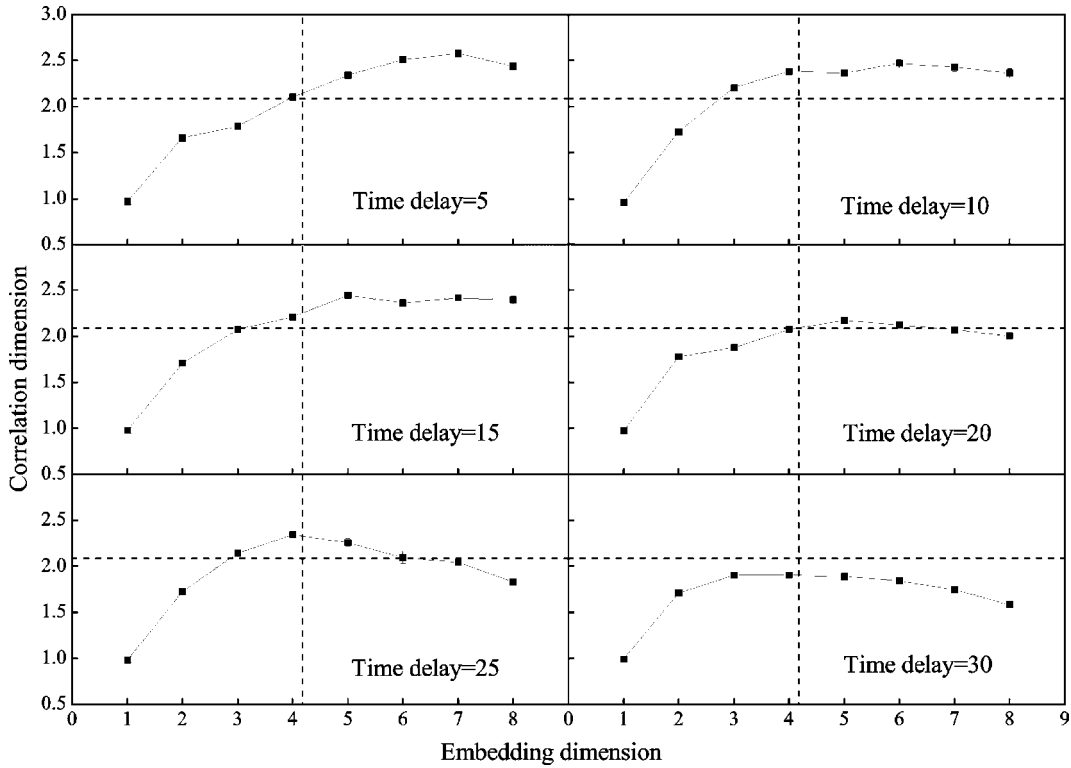


Fig. 2 Correlation dimension D versus the embedding dimension d for the Lorenz model. Each panel has the same scale of D and also the same scale of d .

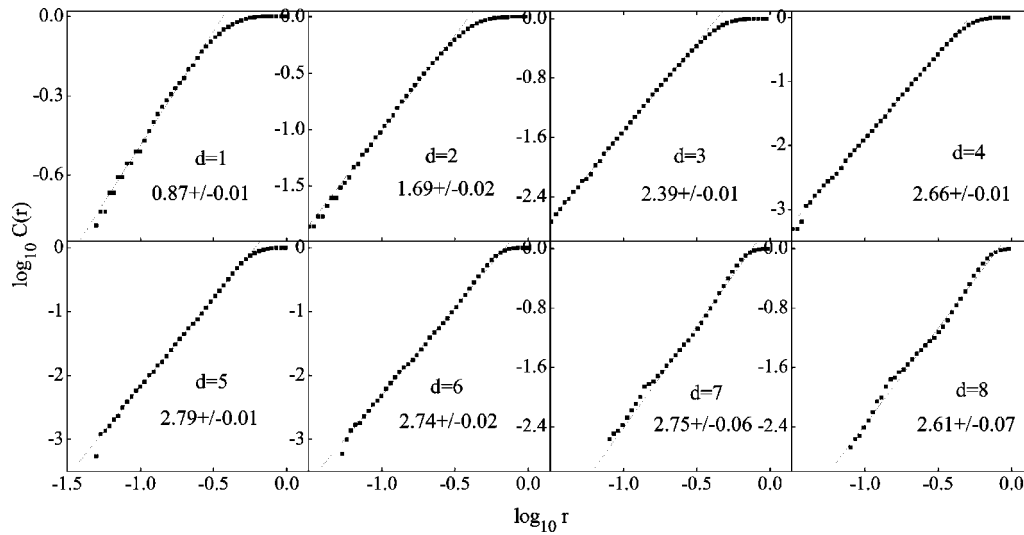


Fig. 3 Correlation integral $C(r)$ of 3C 273 for time delay $T = 30$ and embedding dimension $d = 1, 2, \dots, 8$ on doubly logarithmic scales. In each panel the scale of $C(r)$ is arbitrary and the scale of r is the same. We also give the slope fitted by using Eq. (4) in each panel.

and generate 292 data points representing $x(t)$ at equally spaced time intervals of $\Delta t = 0.05$. Note that the 292 data points are generated from $t = 50$ to ensure the trajectory is on the attractor.

The 292 data points are analyzed using Equations (2) and (4). The results of $\log_{10} C(r)$ plotted against $\log_{10} r$ for time delay $T = 20$ are shown in Figure 1. We can see that in the intermediate region there is approximately a straight line fit. We also plotted $\log_{10} C(r)$ versus $\log_{10} r$ for some other T values and found that the curves are also approximately straight lines in the intermediate region as in Figure 1. Figure 2 shows the correlation dimension D versus embedding dimension d plotted for various time delays T . Now we carefully compare these curves for different T to identify the value of T that makes $d_{\text{sat}} \approx 2D_{\text{sat}}$. We note, when $T = 25$ or 30 , we cannot find a good plateau in the curve. When $T = 5$, d_{sat} is close to 6, and $D_{\text{sat}} \approx 2.508 \pm 0.026$ obtained by averaging the values of correlation dimension for $d = 6, 7, 8$. When $T = 10, 15$ and 20 , d_{sat} is close to 4, and the corresponding $D_{\text{sat}} \approx 2.401 \pm 0.039, 2.367 \pm 0.031$ and 2.088 ± 0.025 obtained by averaging D for $d = 4, 5, 6, 7, 8$. Thus, the best value which makes $d_{\text{sat}} \approx 2D_{\text{sat}}$ is 20. The value of D_{sat} estimated from the curve of $T = 20$ is about 2.088 ± 0.025 . Thus, the attractor dimension is about 2.088 ± 0.025 . Two crossing dash lines representing $D_{\text{sat}} = 2.088$ and $d_{\text{sat}} = 4.176$ are marked in Figure 2. From the two lines, not only can we easily see why $T = 20$ is the special value which we choose to estimate the attractor dimension, but also we find that there is a downward trend in the value of D_{sat} as T increases. By using the full state space vectors and a large amount of data, one can find a more accurate value of the correlation dimension of the Lorenz chaotic attractor, which equals 2.068 ± 0.086 (Sprott 2003). Our result is very close to it.

From the analysis of the Lorenz model, we know that the curve of $\log_{10} C(r)$ versus $\log_{10} r$ is approximately a straight line in the intermediate region for a dissipative system with an attractor. Thus, the correlation dimension can be estimated from the slope of the straight line. Moreover, for the dissipative system, the correlation dimension D will be independent of the embedding dimension d as it increases and a special value of the delay time T which makes $d_{\text{sat}} \approx 2D_{\text{sat}}$ can be identified.

Now we analyze the 292 data points of the light curve of 3C 273 in the form of 100-day means (Kunkel 1967). The results of $\log_{10} C(r)$ plotted against $\log_{10} r$ for time delay $T = 30$ are shown in Figure 3. The curves are also approximately straight lines in the intermediate region, as in Figure 1. The results of correlation dimension D plotted against d for different time delays T are shown in Figure 4. As in Figure 2, when $T = 35$ it is difficult to find a good plateau to estimate the attractor dimension. When

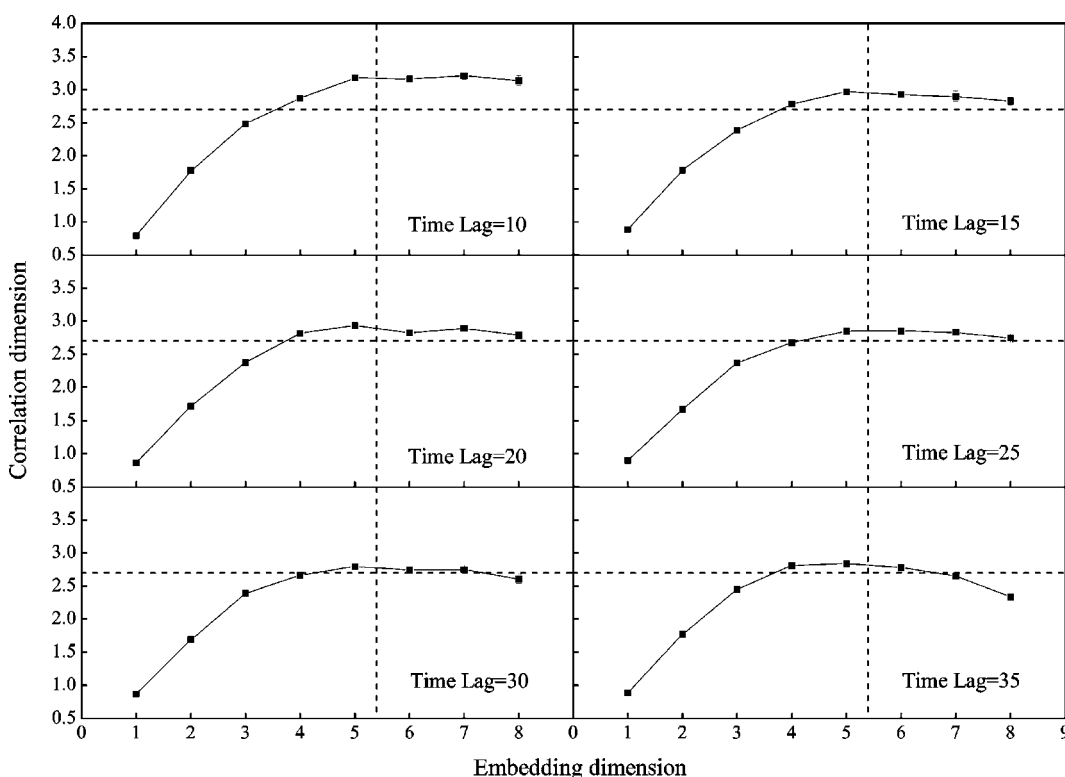


Fig. 4 Correlation dimension D versus the embedding dimension d for 3C 273. Each panel has the same scale of D and also the same scale of d .

$T = 10, 15, 20, 25$ and 30 , d_{sat} is close to 5, and the corresponding $D_{\text{sat}} \approx 3.17 \pm 0.05, 2.90 \pm 0.05, 2.86 \pm 0.04, 2.82 \pm 0.04$ and 2.72 ± 0.04 obtained by averaging D for $d = 5, 6, 7$ and 8 . Thus, the best value which makes $d_{\text{sat}} \approx 2D_{\text{sat}}$ is 30 and the attractor dimension is estimated to be about 2.72 ± 0.04 . Two crossing dash lines in Figure 4 represent $D_{\text{sat}} = 2.7$ and $d_{\text{sat}} = 5.4$. Guided by the two lines, we also readily find why $T = 30$ is special and there is a downward trend in the value of D_{sat} as T increases.

At last, we compare the Lorenz model with 3C 273. First, the curve of $\log_{10} C(r)$ versus $\log_{10} r$ is approximately a straight line in the intermediate region in both. Secondly, a plateau, where the embedding dimension is independent of the correlation dimension, can be found at some values of time delay T both in the Lorenz model and 3C 273. Thirdly, the special time delay T which makes $d_{\text{sat}} \approx 2D_{\text{sat}}$ can be identified in both. Fourthly, there is a downward trend in the value of D_{sat} as T increases in both. These similarities between the two cases strongly suggest that there is a low-dimension chaotic attractor in the light curve of 3C 273.

4 DISCUSSION

The nature of AGNs is still an open question. The study of variations in their light curves is expected to yield valuable information about their nature. 3C 373 has been known to be the brightest AGN. In this paper, the state-space reconstruction and correlation integral are used to analyze the light curve of 3C 273, and the result is compared with the Lorenz model. The similarity between them strongly suggests there is a low-dimension chaotic attractor in the light curve of 3C 273. Thus, the variation of the light curve of 3C 273 has a nonlinear dynamical origin, which cannot be interpreted as multi-periodic behavior or a purely random process. The evidence of chaotic behavior we showed indicates that the concepts of nonlinearity may be helpful to understand the nature of the variations in the light curves of AGNs.

It is interesting to compare 3C 273 with other sources. Misra et al. (2004, 2006) have analyzed the X-ray light curves of GRS 1915+105 by using the same method along with surrogate data analysis and found evidence for a non-linear limit cycle origin for one of the low frequency QPOs detected in the source, while some other types of variability can be due to an underlying low-dimension chaotic system. The chaotic behavior found in the microquasar GRS 1915+105 and the quasar 3C 273 implies that chaotic behavior may be a universal feature in the seemingly random light curves found in many sources. It is expected to find a common nonlinear dynamical origin to explain this chaotic behavior, which may be the nonlinear temporal evolution of the magneto-hydrodynamic flow of the inner accretion disk (Misra et al. 2004, 2006), and it also may come from turbulent motion in a gaseous cloud around the object (Li & Xiao 2000).

Some authors (e.g., Uttley et al. 2005) have considered that dynamical chaos is not required to explain the data, but our results together with Misra et al. (2004) cogently proved that the seemingly random light curves found in some sources are indeed chaotic. We expect that our results are confirmed further by other chaotic and nonlinear time-series analyses.

Acknowledgements The author thanks Professor Meng Ta-Chung for his kind help to understand of non-linear dynamics. Many thanks go to Wang Xiao-Dong and Yu Yun-Wei for improving the manuscript, and to Professor Wang En-Ke for enthusiastic help and encouragement.

References

- Abarbanel H. D. I., Brown R., Sidorowich J. J. et al., 1993, *Rev. Mod. Phys.*, 65, 1331
Fahlman G. G., Ulrych T. J., 1975, *ApJ*, 201, 277
Feder J., 1988, *Fractal*, New York: Plenum
Grassberger P., Procaccia I., 1983, *Phys. Rev. Lett.*, 50, 346
Hilbron R. C., 1994, *Chaos and Nonlinear Dynamics*, Oxford: Oxford University Press
Jurkevich I., 1971, *Ap&SS*, 13, 154
Kunkel W. E., 1967, *AJ*, 72, 1341
Lin R.-G., 2001, *Chin. J. Astron. Astrophys. (ChJAA)*, 1, 245
Lorenz E. N., 1963, *J. Atmos. Sci.*, 20, 130
Li Z.-W, Xiao X.-H, 2000, *Astrophysics*, Beijing: Higher Education Press
Manwell T., Simon M., 1966, *Nature*, 212, 1244
Manwell T., Simon M., 1968, *AJ*, 73, 407
Misra R., Harikrishnan K. P., Mukhopadhyay B. et al., 2004, *ApJ*, 609, 313
Misra R., Harikrishnan K. P., Ambika G. et al., 2006, arXiv: astro-ph/0603281
Packard N. H., Crutchfield J. P., Farmer J. D. et al., 1980, *Phys. Rev. Lett.*, 45, 712
Sprott J. C., 2003, *Chaos and Time-Series Analysis*, Oxford: Oxford University Press
Smith H. J., Hoffleit D., 1963, *Nature*, 198, 650
Sillanpaa A., Haarala S., Korhonen T., 1988, *A&AS*, 72, 347
Terrell J., Olsen K. H., 1970, *ApJ*, 161, 399
Uttley P., McHardy I. M., Vaughan S., 2005, *MNRAS*, 359, 345